IEEE Access
Multidisciplinary | Rapid Review | Open Access Journal

Received June 29, 2019, accepted July 18, 2019, date of publication July 29, 2019, date of current version August 13, 2019.

Digital Object Identifier 10.1109/ACCESS.2019.2931575

An Adaptive Takagi–Sugeno Fuzzy Model-Based Generalized Predictive Controller for Pumped-Storage Unit

JIANZHONG ZHOU, NAN ZHANG, CHAOSHUN LI, (Member, IEEE), YONGCHUAN ZHANG, AND XINJIE LAI

School of Hydropower and Information Engineering, Huazhong University of Science and Technology, Wuhan 430074, China

Corresponding author: Nan Zhang (zhangnanhust@163.com)

This work was supported in part by the National Key Research and Development Program of China under Grant 2016YFC0402205, in part by the National Natural Science Foundation of China under Grant 51679095 and Grant 51879111, and in part by the State Grid Xin Neng Yuan Ltd. (State Grid New Energy Ltd.).

ABSTRACT In order to improve the control performance and suppress the "S" characteristics area instability of the pumped-storage unit (PSU), this paper proposes an adaptive Takagi–Sugeno fuzzy model-based generalized predictive controller (ATS-GPC) for the PSU. First, the T–S fuzzy model is used to obtain the controlled autoregressive integrated moving average (CARIMA) model, in which the fuzzy C-means (FCM) clustering algorithm is used for the identification of antecedent parameters and the least square method (LSM) is used to obtain the consequent parameters. Meanwhile, the T–S fuzzy model can be online adjusted according to the real-time tracking error feedback to decrease the influence of the initial offline trained fuzzy model. Then, the generalized predictive controller is designed for the PSU based on the CARIMA. Finally, some numerical simulation experiments including the start-up process, frequency disturbance process, frequency tracking experiments, and robustness analyses have been conducted to verify the proposed method. The experiments results have shown that the proposed ATS-GPC can significantly improve the control performance of the PSU and effectively suppress the unstable operation in "S" characteristics area. In addition, the strong robustness of the proposed controller is verified.

INDEX TERMS Adaptive, T-S fuzzy model, generalized predictive controller, pumped-storage unit, pump turbine governing system, "S" characteristics area.

I. INTRODUCTION

Recently with the rapid development of human society, such problem as the traditional energy shortage, environment pollution have become more and more severe, so realizing the transition from fossil energy system to clean and renewable energy system is an effective approach to climate and environment change [1]–[3]. The wind energy [4], [5] and solar [6], [7] energy which are important renewable energy sources have attracted more attention due to the availability and abundant reserves. However, the problem of intermittent and randomness fluctuations of the wind and solar energy still need to be addressed, which will bring a great negative impact on the safety and stability of the power system. The energy storage technology is an effective tool to solve this problem, which has always become the research hotspot. Pumped storage is not only the important clean renewable energy, but also is an effective large-scale power storage tool, which has currently become the most commonly used complementary energy for wind and solar energy [8], [9]. Therefore the speeding up the construction of pumped storage power station (PSPS) is an important measure for improving the ecological environment and the safety and stability of the power system.

The control technologies of the pumped turbine governing system (PTGS) are facing more and more challenges with the rapid development of the PSPS and the higher head and larger unit capacity PSU being adopted [10], [11]. The PSU which is designed to work at both pump and turbine modes with opposite flow and rotating directions has more operating

The associate editor coordinating the review of this manuscript and approving it for publication was Ramesh Babu N.

conditions and conditions conversion. The researches have shown that the control of PSU is more complicate than the traditional hydroelectric generating unit [12] due to its reversible design and more conditions conversion. The complete characteristics curves which are used to describe the steady state characteristics of the pump-turbine show typical ''S'' characteristics area caused by its reversible design [13], [14]. In the region of ''S'' characteristics, there exist strong guide vane opening curves cross, aggregation and twisting phenomenon in the two ends of the curves, so one unit speed value corresponds to three unit flow values or three unit torque [15]. The pump-turbine will can't guarantee sable operation and even may switch back and forth between the turbine conditions, the turbine braking conditions and the reverse pump conditions when it runs into the ''S'' characteristics area. The reversible pump-turbine is apt to fall into the ''S'' characteristics area under no-load turbine start-ups connected to the power grid in low water head [16] and turbine load rejections [17]. The ''S'' characteristics have brought more difficulties for the control of the PSU, therefore the design of the more effective controller for improving the control performance and avoiding it running into the ''S'' characteristics area becoming increasingly important.

Advanced intelligent controllers are widely used to improve the control performance and suppress the influence of the ''S'' characteristics. Despite the fact that the traditional PID controller has been studied and applied in various fields, but there still exist some deficiencies when it comes to complex conditions. So some new control strategies including fractional-order PID controller [18], [19], sliding mode controller [20], [21], fuzzy control [22]–[24], model predictive control [25], [26] etc. have been proposed and applied in the PTGS. Xu *et al.* designed an adaptively fast fuzzy fractional-order PID control method for PSU using improved gravitational search algorithm (GSA) and obtained better control effect at low and medium water head [19]. Further, Xu *et al.* designed an adaptive condition predictive-fuzzy PID controller, which combines the model predictive control (MPC) and fuzzy logic control theory to study the optimal control of PSU under no-load start-up condition at low head area [26]. Li *et al.* designed of a fractional-order PID controller for a PSU using a gravitational search algorithm based on the Cauchy and Gaussian mutation, which effectively improves the control performance of the PSU at different water head [18]. MPC is the extension of the global optimization control, where the many times finite horizon rolling optimization is used to instead of the once infinite horizon optimization. The control signal of the MPC is adjusted by predicting the system future behaviors. The MPC strategy composed of output predictive, rolling optimization and feedback revision has been proved to be very effective. The generalized predictive control (GPC) method which is the typical MPC has been widely applied to petrochemical industry and other fields [27]–[30].

Although the GPC is a competitive control method for the real-world control problems because of its robustness and disturbance rejection properties, there exist still some problems needed to be solved when it is applied in the complicate nonlinear PTGS. How to obtain the linear inner model of the GPC is a key point. To obtain the inner model of the GPC, the neural network nonlinear autoregressive with exogenous signal (NNARX) was also applied in model identification of elastic and inelastic hydro power plant [31]. Li *et al.* proposed a nonlinear GPC for a PSU, where the parameters of the CARIMA model is obtained online by the recursive least square method [25]. The Takagi–Sugeno (T–S) fuzzy model which is composed of several linear model and can be considered as the time-varying linear model has been successfully applied in the GPC due to its higher modelling accuracy and retaining more linear model advantages [32]–[35].

Inspired by above researches, an adaptive T-S fuzzy model-based GPC (ATS-GPC) is proposed for a PSU. In order to improve the control performance and decreasing the error of the initial offline trained fuzzy model, the adaptive T–S fuzzy model composed of the offline model training and the online consequent parameters adjustment is integrated with the GPC to control a PSU. At a specified sample time, the overall linear model can be obtained by combining the each sub-model by the fuzzy inference. And then the control signal can be calculated according to the optimization method of the GPC. Some experiments including the start-up process, frequency disturbance process, frequency tracking experiments and robustness analyses under different water head have been conducted to verify the proposed method compared with the traditional PID controller. The experiments results have shown that the proposed ATS-GPC can significantly improve the control performance under different water head and avoid the PSU trapping into the ''S'' characteristics area. In addition, the strong robustness of the proposed controller is testified.

The remainder of this paper is organized as follows: Section II describes the accurate model of the pump-turbine governing system. In section III, the adaptive T-S fuzzy model-based generalized predictive controller is proposed. Section IV shows the experimental results of this study. Section V presents the conclusion of this study

II. MODELING OF PUMP TURBINE GOVERNING SYSTEM

The PTGS, as the important control system for the pump-turbine, is mainly employed to adjust the frequency and output power of the PSU and ensure safe and stable operation of the power grid. It is a complex nonlinear and non-minimum phase system mainly consisted of pressure water supply system, pump-turbine, surge tank, speed governor, electrohydraulic servo system, synchronous generator and power grid load, where mechano-electric dynamics and hydrodynamics are all involved [36]–[39]. Therefore the accurate modeling of the PTGS is still an important issue until now. Most of the researches have been done for the modeling of the PTGS. Among these researches, the modeling of the pressure water supply system and the pump-turbine have attracted more attention due to its higher complex characteristics. So in this

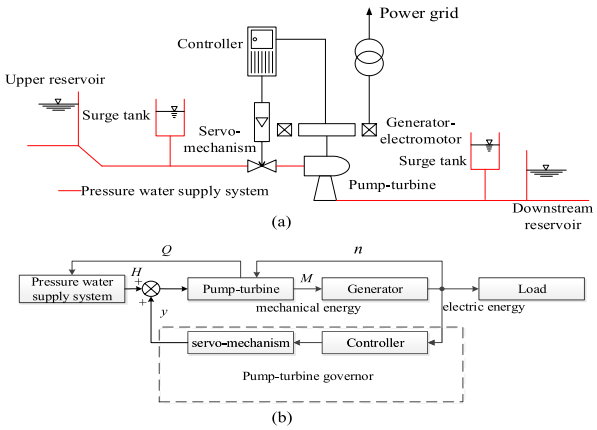

FIGURE 1. Structure of pump-turbine governing system.

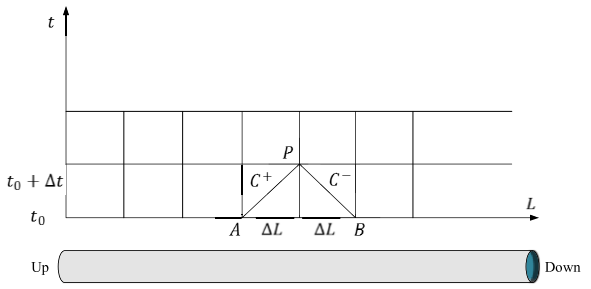

FIGURE 2. Schematic diagram of the MOC.

section, the modeling of the pressure water supply system and the pump-turbine will be emphasized in the following. The structure and the block diagram of the PTGS is shown in Fig. 1.

A. MODELING OF PRESSURE WATER SUPPLY SYSTEM

The hydraulics fundamental equations consisted of a momentum equation and a continuity equation are applied to describe the fluid flow characteristics of the pressure water supply system [40]–[42]:

$$\begin{cases} \textit{Momentum equation}: \dfrac{\partial H}{\partial X} + \dfrac{1}{gA}\dfrac{\partial Q}{\partial t} + \dfrac{fQ|Q|}{2gDA^2} = 0 \\ \textit{Continuity equation}: \dfrac{\partial Q}{\partial X} + \dfrac{gA}{c^2}\dfrac{\partial H}{\partial t} = 0 \end{cases} \tag{1}$$

where A, D and f are the cross-section area, diameter and friction coefficient of the pipeline, respectively. G and t are the gravity acceleration content and time. H and Q are water pressure and flow in the pipeline, respectively. c is pressure wave velocity and the X is the displacement of distance from the reference point. In this paper, the method of characteristics (MOC) is used to establish an accurate model of the pressure water supply system [43].

A pipeline with total length L shown in Fig. 2 can be divided into N equal sections, and the length of each section is $\Delta r = L/N$. At time t, if we know the Q and H at the A and B, the Q and H at time $t + \Delta t$ of the middle point P can be obtained.

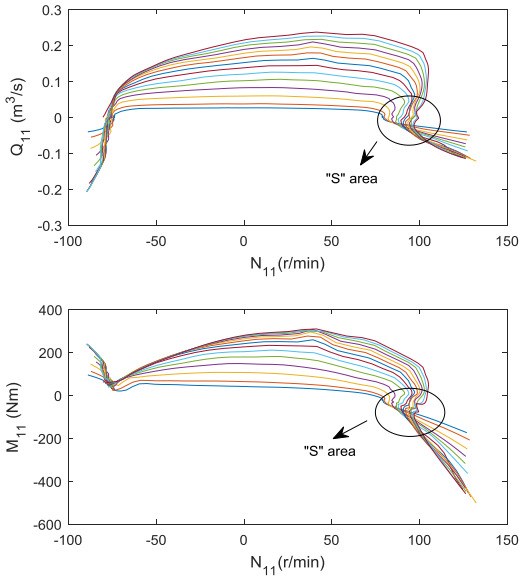

FIGURE 3. Complete characteristic curve of a pump-turbine.

After derivation, the MOC is described as:

$$\begin{cases} C^+ : Q^P_{t+\Delta t} = C_m - C_a H^P_{t+\Delta t} \\ C^- : Q^P_{t+\Delta t} = C_n + C_a H^P_{t+\Delta t} \end{cases} \tag{2}$$

$$\begin{cases} C_m = Q^A_t + C_a H^A_t - C_f Q^A_t |Q^A_t| \\ C_n = Q^B_t - C_a H^B_t - C_f Q^B_t |Q^B_t| \end{cases} \tag{3}$$

where $C_a = gA/c$, $C_f = f\Delta t/2DA$. The Q and H at time $t + \Delta t$ of the middle point P can be obtained by the Eq. (4):

$$\begin{cases} Q^P_{t+\Delta t} = \dfrac{1}{2}(C_m + C_n) \\ H^P_{t+\Delta t} = \dfrac{1}{2}(C_m - C_n) \end{cases} \tag{4}$$

B. MODELING OF PUMP-TURBINE

Pump-turbine is the most important component of the PTGS, although a lot of researches on the modeling of pump-turbine have been conducted, the accuracy analytic expression can't be obtained due to its complicated characteristics. The complete characteristics curves model is often used to establish the accuracy pump-turbine model. The complete characteristics curves of a certain pump-turbine are shown in Fig.3.

The complete characteristics curves consisted of the flow characteristic curves and the torque characteristics curves are applied to describe the nonlinear function of the unit flow Q_{11} and the unit torque M_{11} with respect to the guide vane opening y and unit speed N_{11}. The unit torque and the unit flow characteristic curves are usually provided by the pump-turbine manufacturers in the form of two discrete data tables. Based on the data tables, the unit torque and the unit flow can be obtained by interpolation or nonlinear function fitting.

From the Fig 3, it can be noticed that complete characteristic curves of the pump-turbine exhibit strong guide vane opening curves cross, aggregation and twisting phenomenon in the two ends of the curves called "S" characteristics area.

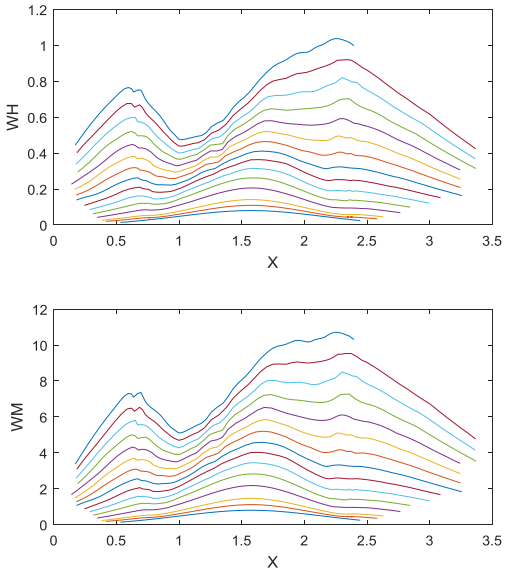

FIGURE 4. Suter transform diagram of characteristics curves of a pump-turbine.

In the "S" area one unit speed value corresponds to three unit flow values of Q_{11} or three unit torque of M_{11}. Such a multiple-value problem will bring some difficulties in application these curves to the modeling of the pump-turbine.

In order to solve these problems, some methods have been proposed, among these methods the Suter transformation method has attracted more attention. Though the Suter transformation is able to solve the multiple-value problem to a certain extent, there are still some deficiencies. So an improved Suter transformation is proposed to overcome these drawbacks [25]:

$$\begin{cases} WH(x,y) = \dfrac{h}{a^2+q^2+C_h\cdot h}(y+C_y)^2 \\ WM(x,y) = (\dfrac{m+k_1 h}{a^2+q^2+C_h\cdot h})(y+C_y)^2 \\ x = \arctan[(q+k_2\sqrt{h})/a] \quad a>0 \\ x = \pi + \arctan[(q+k_2\sqrt{h})/a] \quad a<0 \end{cases} \tag{5}$$

where, $k_2 = 0.5 \sim 1.2$, $C_y = 0.1 \sim 0.3$, $C_h = 0.4 \sim 0.6$. A transformed WH and WM curves based on the improved Suter transformation method have been shown in Fig. 4. It is obvious that the improved Suter transformation method is able to suppress the phenomenon of strong guide vane opening curves cross, aggregation and twisting of the curves.

C. SIMULATION OF PTGS

In order to obtain the accurate simulation result, the iteration calculation is used to obtain the flow Q_{k+1} and unit speed

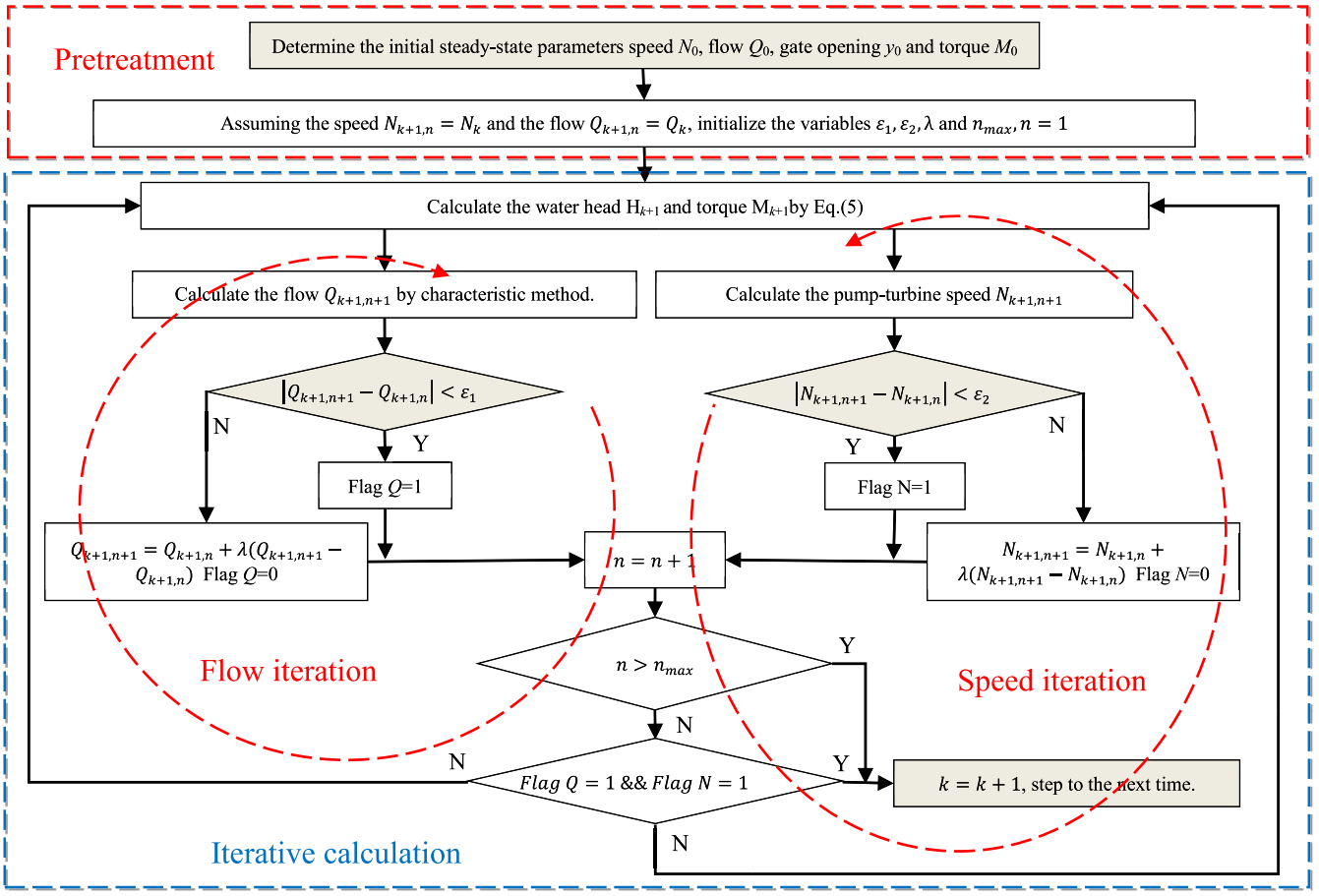

FIGURE 5. The water flow and turbine speed calculation of the PTGS.

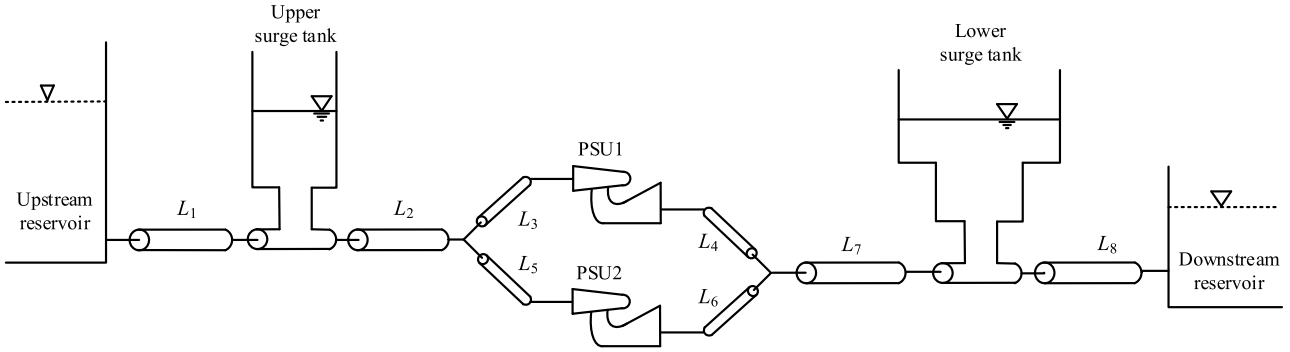

FIGURE 6. Layout diagram of the considered PSPS.

TABLE 1. PSU parameters.

Parameters	Values
High pressure side diameter of turbine runner(m)	3.85
Low pressure side diameter of turbine runner(m)	1.93
Rated speed nr (r/min)	500
Rated water-head Hr (m)	540
Max water-head Hr (m)	565
Min water-head Hr (m)	526
Rated water flow Qr (m3/s)	62.09
Power rating P (MW)	306.1
Moment of inertia M (ton/m2)	3800
100% guide-vane opening ymax (°)	20.47
Water level of the upstream reservoir Hu (m)	730.4
Water level of the downstream reservoir Hd (m)	168.5

TABLE 2. Surge tank parameters.

Parameters	Elevation(m)	Area(m^2)	Impedance Area(m^2)	Inflow loss coefficient	Outflow loss coefficient
Upper surge tank	678.49-687.50	12.57	12.57	0.001475	0.00108
	688.50-757.00	63.62			
	91.10-130.00	15.90			
Low surge tank	130.00-189.00	95.03	15.90	0.000921	0.00067
	189.00-195.50	519.98			

N_{k+1} of the next time $k+1$ for the simulation of the PTGS, as shown in the flowchart of Fig. 5.

D. MODEL VALIDATION: COMPARISON OF SIMULATION AND MEASUREMENTS

In this section, in order to validate the rationality and accuracy of the established PTGS model, the simulation and the on-site measurements results are compared, where a real PSPS is considered. The layout diagram of the pressure water supply system is presented in Fig. 6, which is the typical "one pipeline – double units" PSPS. The detailed PSPS parameters are listed in Table 1–4. In this case study, the single PSU load rejection simulation experiment is considered. The simulation results are compared with the on-site measurements, shown in Fig. 7. Fig. 7 show that the simulation results achieve a reasonable agreement with the on-site measurement, especially during the first extremums of rotational speed, water pressure in the volute and the draft tube.

III. ADAPTIVE T-S FUZZY MODEL-BASED GENERALIZED PREDICTIVE CONTROLLER DESIGN

In this section, an adaptive T-S fuzzy model-based generalized predictive control (ATS-GPC) is designed, where the adaptive T-S fuzzy model is applied to replace the original nonlinear plant.

A. DERIVATION OF THE GENERALIZED PREDICTIVE CONTROL LAW

The GPC, as one of the typical MPC algorithms, has the same three basic characteristics: predictive model, rolling optimization and feedback revision. The predictive model is considered as the approximate model of the original nonlinear plant to predict the original system output and compute the current optimal control signal. To establish the GPC algorithm, the CARIMA model structure is used to approximate the dynamic behaviour of the original nonlinear system. The basic structure of the CARIMA can be written as

TABLE 3. Pipeline parameters.

Pipeline	Length(m)	Diameter(m)	Area	Wave velocity(m/s)
1	444.23	6.20	30.1578	1094.16
2	865.69	5.04	19.9688	1189.33
3	117.86	2.6	5.2909	1202.65
4	155.4	4.19	13.7985	1110
5	108.36	2.57	5.1698	1290
6	165.9	4.2	13.884	1077.27
7	15	6.5	33.1814	1071.43
8	1065.2	6.58	33.9712	1001.13

TABLE 4. Parameters of the simulated model of PTGS.

object	value			
Suter-transformation	k1=10	k2=0.9	Cy=0.2	Ch=0.5
Generator	Ta=8.503	eg=0		
Servo-mechanism	Ty_b=0.05	Ty=0.3	k0=1	
Simulation setting	ts=0.08s			

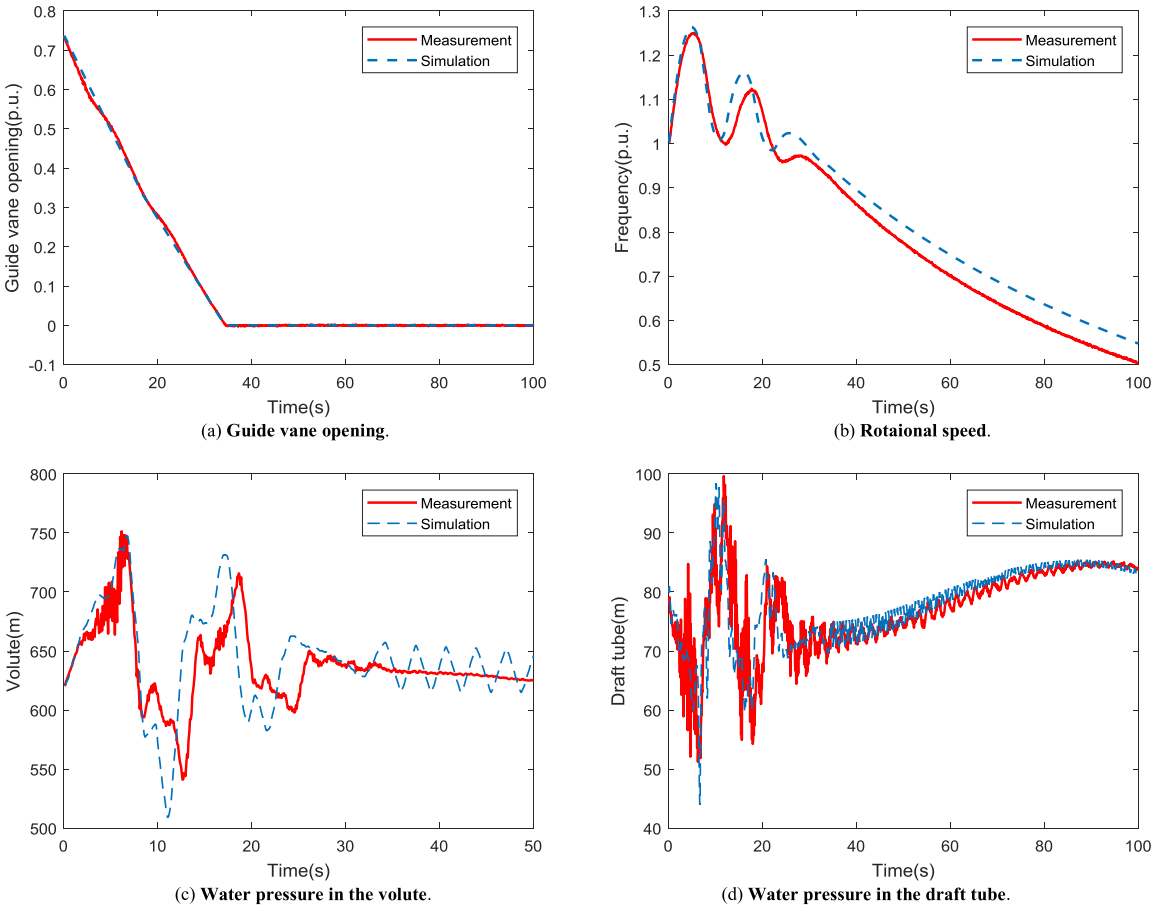

(a) **Guide vane opening**. (b) **Rotaional speed**. (c) **Water pressure in the volute**. (d) **Water pressure in the draft tube**.

FIGURE 7. Simulation results compared to on-site measurements during a load rejection.

follows [44], [45]:

$$A(z^{-1})y(k) = z^{-d}B(z^{-1})u(k) + C(z^{-1})\xi(k)/\Delta \tag{6}$$

where $u(k)$ is the control signal, $y(k)$ is the controlled plant output, $\xi(k)$ is an white noise sequence set, d is the system delay time. $\Delta = 1 - z^{-1}$ is the difference operator, and $A(z^{-1})$, $B(z^{-1})$, $C(z^{-1})$ are the polynomials and defined as follows:

$$\begin{cases} A(z^{-1}) = 1 + a_1 z^{-1} + a_2 z^{-2} + \cdots + a_{n_a} z^{-n_a} \\ B(z^{-1}) = b_0 + b_1 z^{-1} + b_2 z^{-2} + \cdots + b_{n_b} z^{-n_b} \\ C(z^{-1}) = 1 + c_1 z^{-1} + c_2 z^{-2} + \cdots + c_{n_c} z^{-n_c} \end{cases} \tag{7}$$

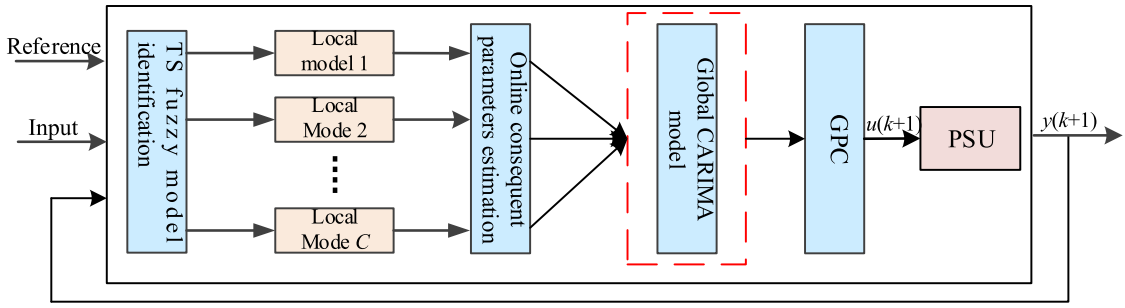

FIGURE 8. Structure of the adaptive fuzzy model-based predictive controller for PSU.

Combined Eq. (6) and Eq. (7), the output predictive model with $C(z^{-1}) = 1$ can be derived:

$$y(k+j) = F_j \Delta u(k+j-1) + G_j y(k) + E_j \xi(k+j) \quad (8)$$

According to Eq. (8), the matrix form of the output predictive model of the system can be written as follows:

$$\begin{aligned} Y &= F_1 \Delta U + F_2 \Delta U(k-j) + GY(k) + E\xi \\ &= F_1 \Delta U + Y_1 + E\xi \end{aligned} \quad (9a)$$

where:

$$\begin{cases} Y_1 = F_2 \Delta U(k-j) + GY(k) \\ Y = [y(k+N_1), y(k+N_1+1), \cdots, y(k+N_2)]^T \\ \Delta \mathrm{U} = [\Delta u(k), \Delta u(k+1), \cdots, \Delta u(k+N_u-1)]^T \\ \Delta U\,(k-j) = [\Delta u(k-1), \Delta u(k-2), \cdots, \Delta u(k-n_b)]^T \\ Y\,(k) = [y\,(k)\,, y\,(k-1)\,, \cdots, y\,(k-n_a)]^T \\ \xi = [\xi(k+1), \xi(k+2), , \xi(k+N_2)]^T \end{cases} \quad (9b)$$

where the positive integers N_1, N_2 and N_u are the minimum predictive horizon, maximum predictive horizon and control horizon, respectively.

The GPC algorithm, as one of the optimized control algorithms, the control law is formulated by minimizing a certain performance index. The most of used performance index is considered:

$$\mathrm{J} = \min \left\{ \sum_{j=N_1}^{N_2} [y\,(k+j) - y_r\,(k+j)]^2 + \sum_{j=1}^{N_u} [\gamma_i \Delta u(k+j-1)]^2 \right\} \quad (10)$$

The First Order Lag model is used to create the reference trajectory of the output of the system:

$$\begin{cases} y_r(k) = y(k) \\ y_r(k+j) = \alpha y_r(k+j-1) + (1-\alpha) w \end{cases} \quad (11)$$

where $y(k)$ is the actual output of the system at k_{th} step, $y_r(k)$ is the setting point of system, α is the smoothing factor.

TABLE 5. Working conditions.

Condition number	Upper water level	Downstream water level	Working head
T1	735.45 m	181 m	554 m
T2	735.45 m	189 m	546 m
T3	716 m	181 m	535 m

TABLE 6. Parameters of controllers under start-up process.

Controller	Controller arameters			
PID	$K_p = 3.97$	$K_i = 1.41$	$K_d = 9.64$	\
	$K_p = 4.08$	$K_i = 1.32$	$K_d = 9.82$	\
	$K_p = 4.11$	$K_i = 1.04$	$K_d = 9.21$	\
ATS-GPC	$N_2 = 37$	$N_u = 17$	$\alpha = 0.92$	$\gamma = 100$
	$N_2 = 37$	$N_u = 17$	$\alpha = 0.92$	$\gamma = 100$
	$N_2 = 37$	$N_u = 17$	$\alpha = 0.92$	$\gamma = 100$

For convenience, this performance index Eq. (10) can be written in a compact form:

$$\begin{cases} J = \min\{[^Y[Y - Y_r]^T[Y - Y_r] + \Delta U^T \Gamma \Delta U\} \\ Y_r = [y_r(k+N_1), y_r(k+N_1+1), \cdots, y_r(k+N_2)]^T \\ \Gamma = diag(\gamma_1, \gamma_2, \cdots, \gamma_{N_u}) \end{cases} \quad (12)$$

where $\mathbf{Y}_\mathrm{r}$ is the reference trajectorie of system.

Inserting Eq. (9) to Eq. (12), we can get:

$$J = \min\{[Y - Y_r]^T[Y - Y_r] + \Delta U^T \Gamma \Delta U\} \quad (13)$$

For the unconstrained GPC algorithm, the optimal solution can be explicitly obtained by setting the gradient of the performance index J to zero, the control increment vector could be calculated:

$$\Delta U(k) = (F_1^T F_1 + \Gamma)^{-1} F_1^T [Y_r - F_2 \Delta U(k-j) - GY(k)] \quad (14)$$

To avoid the control error due to the model mismatch and environmental disturbance, the current control variable $u(k)$ is used instead of the entire control vector, so the current control variable could be defined as follows:

$$u(k) = u(k-1) + [1, 0, \cdots, 0] \Delta U(k) \quad (15)$$

B. T-S FUZZY MODEL

The predictive model of the GPC algorithm in terms of CARIMA form has been described above. It is obvious that

TABLE 7. Performance indicators of the simulated PSU with different controller in start-up process.

Condition number	Controller	Performance measure of rotational speed			
		ITAE	OS(%)	ST(s)	SSE(%)
T1	PID	2406.80	3.07	44	0.08
	ATS-GPC	**2328.27**	**0.27**	**33.76**	**0.01**
T2	PID	2448.82	2.91	44	0.26
	ATS-GPC	**2352.95**	**0.26**	**33**	**0.26**
T3	PID	2498.28	2.60	44	**0.03**
	ATS-GPC	**2420.67**	**0.19**	**33.36**	0.18

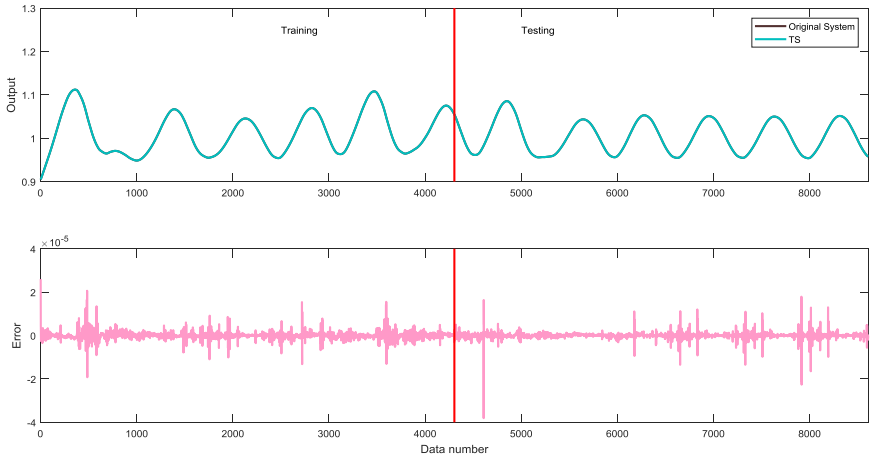

FIGURE 9. Comparison of T-S fuzzy model and original system for the PTGS.

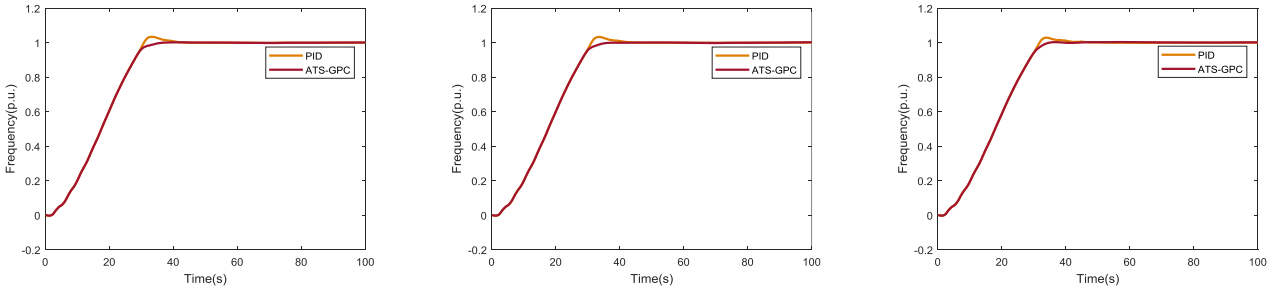

(a) **Hw = 554 m** (b) **Hw = 546 m** (c) **Hw = 535 m**

FIGURE 10. Rotational speed curves of the PSU with different water heads in start-up process.

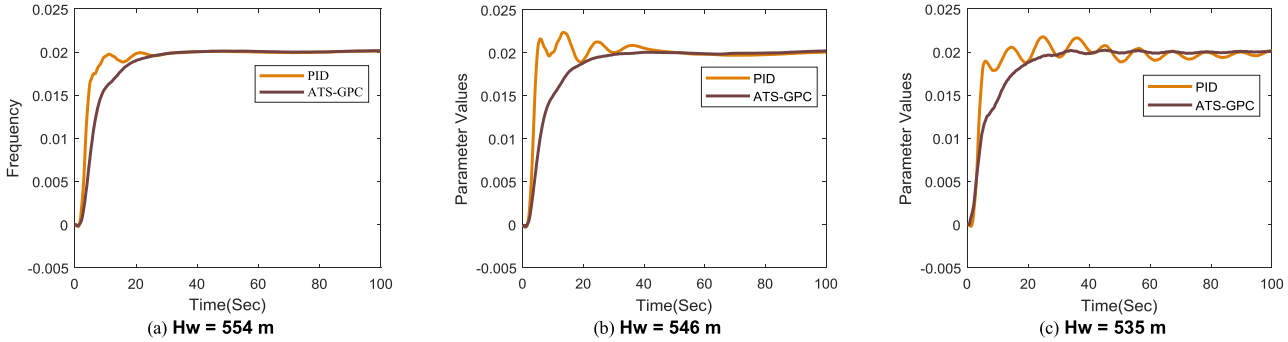

(a) **Hw = 554 m** (b) **Hw = 546 m** (c) **Hw = 535 m**

FIGURE 11. Rotational speed curves of the PSU with different water heads in speed disturbance process.

the CARIMA model is a linear model, but most of the controlled plants are complex nonlinear. Therefore the standard GPC algorithm is not suitable for nonlinear plants. To solve this problem and extend the field of the GPC algorithm, some modeling methods have been proposed to establish the predictive model of the GPC algorithm.

The T-S fuzzy model, as one of the data-driven modeling methods, has been widely applied in problem of nonlinear

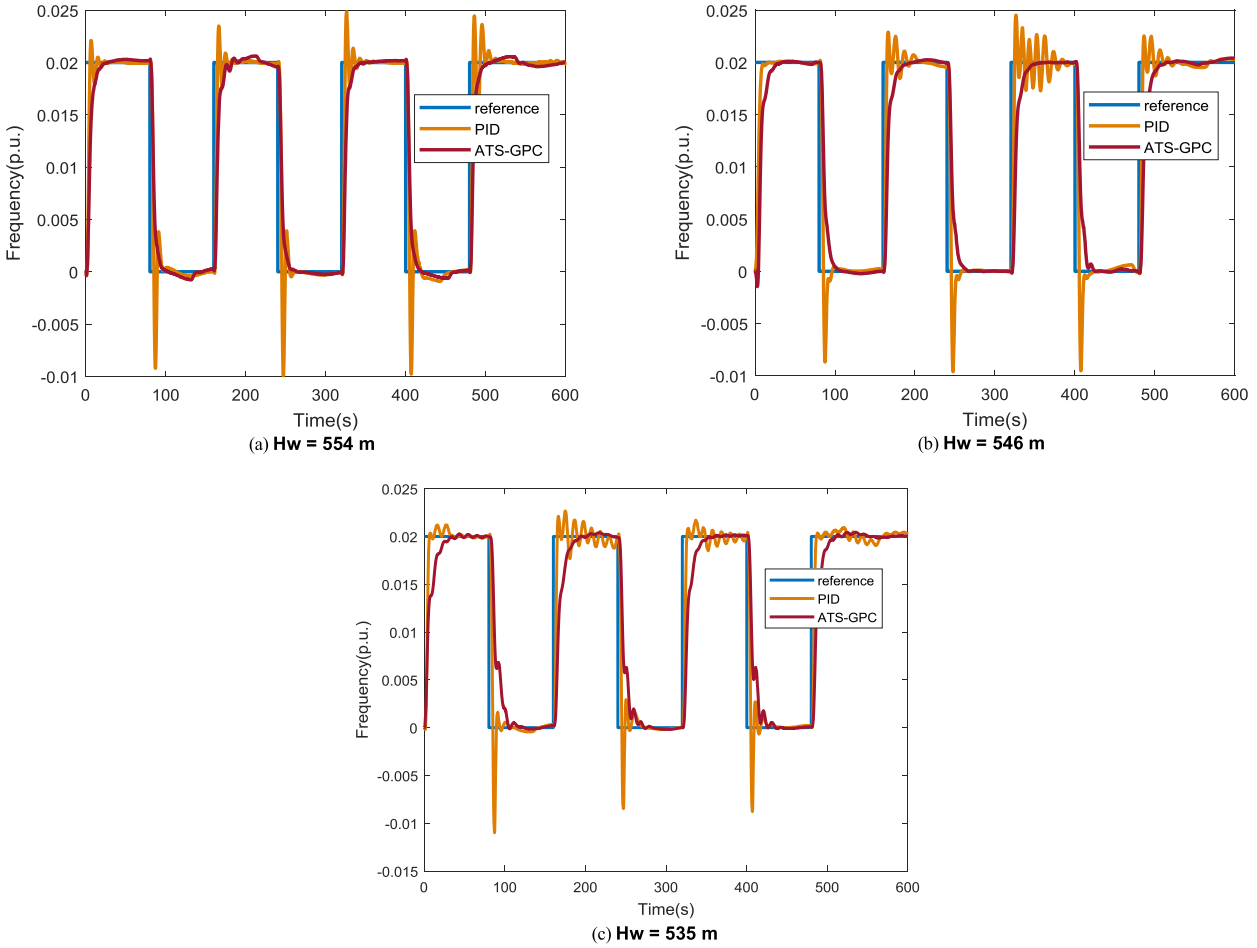

FIGURE 12. Rotational speed curves of the PSU with different water heads in step signal tracking process.

system identification due to its simple, interpretable structure and universal approximation ability [46]–[48]. The remarkable advantage is that the T-S fuzzy model is the weighted synthesis of several local linear models and retains a lot of advantages of the linear model. So the nonlinear system modeling based on the T-S fuzzy model can be considered as a time-varying linear system. It provides more convenience for the design of the GPC.

Considering a multi-input single-output (MISO) system, the T-S fuzzy model of this system can be described by the following IF-THEN fuzzy rules:

Rule R_i: IF x_1 is A_1^i and $\ldots$ and x_M is A_M^i THEN

$$y^i = \theta_0^i + \theta_1^i x_1 + \cdots + \theta_M^i x_M \tag{16}$$

where $R_i (i = 1, 2, \ldots, c)$ is the i_{th} fuzzy rule, c is the number of fuzzy rule. $x = [x_1, x_2, \ldots, x_m]$ is the input variable of the fuzzy model, M is the dimension of the x. y^i is the output of the sub-model belonging to the i_{th} rule, and $\{\theta_j^i, j = 0, \ldots, M\}$ is the consequent parameter of i_{th} sub-model.

The final output of T-S fuzzy model is comprised of those sub-models as a form of weighted mean defuzzification:

$$y = \frac{\sum_{i=1}^{c} w^i y^i}{\sum_{i=1}^{c} w^i} \tag{17}$$

TABLE 8. Parameters of controllers under frequency disturbance process.

Controller	Controller arameters			
PID	$K_p = 2.10$	$K_i = 0.66$	$K_d = 1.74$	\
	$K_p = 2.01$	$K_i = 1.02$	K_d =4.45	\
	$K_p = 1.72$	$K_i = 0.81$	K_d =4.64	\
ATS-GPC	$N_2 = 50$	$N_u = 17$	α =0	γ = 200
	$N_2 = 50$	$N_u = 7$	α =0.6	γ = 200
	$N_2 = 37$	$N_u = 7$	α =0.95	γ = 200

where the weight w^i denotes the overall membership grade of input $\mathbf{x}$ belonging to the i_{th} sub-model. It can be calculated as:

$$\mathrm{w^i} = \prod_{\mathrm{j}=1}^{\mathrm{M}} \mu_{\mathrm{A_j^i}}(\mathrm{x_j}) \tag{18}$$

where $\mu_{A_j^i}(x_j)$ is fuzzy membership grade of x_j belonging to fuzzy set A_j^i.

C. GPC ALGORITHM COMBINE WITH T-S FUZZY MODEL IDENTIFICATION

The CARIMA model parameters estimation based on the T-S fuzzy model identification will be discussed in this part.

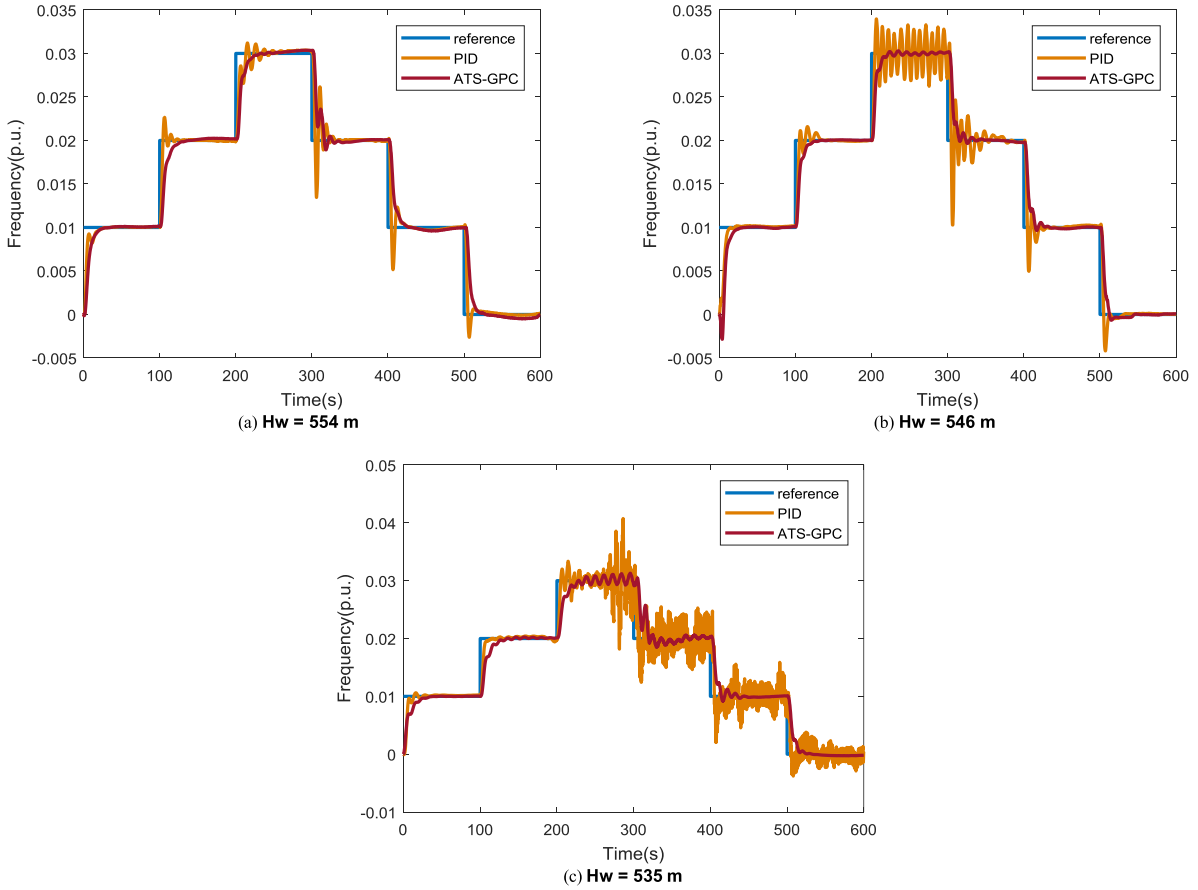

FIGURE 13. Rotational speed curves of the PSU with different water heads in step signal tracking process.

Considering the situation $C(z^{-1}) = 1$, the CARIMA model can be transformed to be:

$$\begin{aligned}\Delta y(k) &= [1 - A(z^{-1})]\Delta y(k) + B(z^{-1})\Delta u(k-1) + \xi(k) \\ &= -\sum_{j=1}^{n_a} a_j \Delta y(k-j) + \sum_{j=1}^{n_b} b_j \Delta u(k-j) + \xi(k)\end{aligned} \tag{19}$$

If the input variable of the fuzzy model x is consisted of control inputs increment and outputs increment of the original system, the Eq. (16) can be expressed as following form:

$$\Delta y_i(k) = \sum_{j=1}^{n_a} -a_{ij}\Delta y(k-j) + \sum_{j=1}^{n_b} b_{ij}\Delta u(k-j) \tag{20}$$

At a certain a sample time, if input $\mathbf{x}$ has been obtained, the weight w^i can be calculated and the output of the system is defined:

$$\Delta y(k) = \sum_{i=1}^{c} \omega_i \Delta y_i(k) \tag{21}$$

where $\omega_i = w^i / \sum_{i=1}^{c} w^i$

Inserting the Eq. (21) into Eq. (20):

$$\begin{aligned}&\Delta y(k) \\ &= \sum_{j=1}^{c} \omega_i \Big(\sum_{j=1}^{n_a} -a_{ij}\Delta y\,(k-j) + \sum_{j=1}^{n_b} b_{ij}\Delta u(k-j)\Big) \\ &= -\sum_{j=1}^{n_a} -a_j \Delta y\,(k-j) + \sum_{j=1}^{n_b} b_j \Delta u(k-j)\end{aligned} \tag{22a}$$

where a_j and b_j are define as

$$\begin{cases} a_j = \sum_{i=1}^{c} \omega_i a_{ij} \\ b_j = \sum_{i=1}^{c} \omega_i b_{ij} \end{cases} \tag{22b}$$

Compared the Eq. (19) and the Eq. (22), we can find that the T-S fuzzy model and the CARIMA model have similar model structure if the input variable of the fuzzy model is chosen properly. So the T-S fuzzy model identification method can be used to establish the CARIMA model. But the T-S fuzzy model of the nonlinear system may not be well trained initially, so the consequent parameters of the sub-model need to be adjusted adaptively according to the actual system output, this is called the feedback revision. $\hat{\theta} = [\theta_1^0, \ldots, \theta_1^m, \ldots, \theta_c^0, \ldots, \theta_c^m]$ is the fuzzy model consequent parameters to be on-line estimated by the recursive least squares method:

$$\begin{cases} \hat{\theta}(k) = \hat{\theta}(k-1) + K(k)[\Delta y(k) - \varphi^T(k)\hat{\theta}(k-1)] \\ K(k) = \dfrac{P(k-1)\varphi(k)}{\lambda + \varphi^T(k)P(k-1)\varphi(k)} \\ P(k) = \dfrac{1}{\lambda}[I - K(k)\varphi^T(k)]P(k-1) \end{cases} \tag{23}$$

where $\varphi(k) = [1, \lambda_1^k x_{k1}, \ldots, \lambda_1^k x_{km}, \ldots, 1, \lambda_N^k x_{k1}, \ldots, \lambda_N^k x_{km}]$, $P(k)$ is the covariance matrix, $K(k)$ is the adjustment

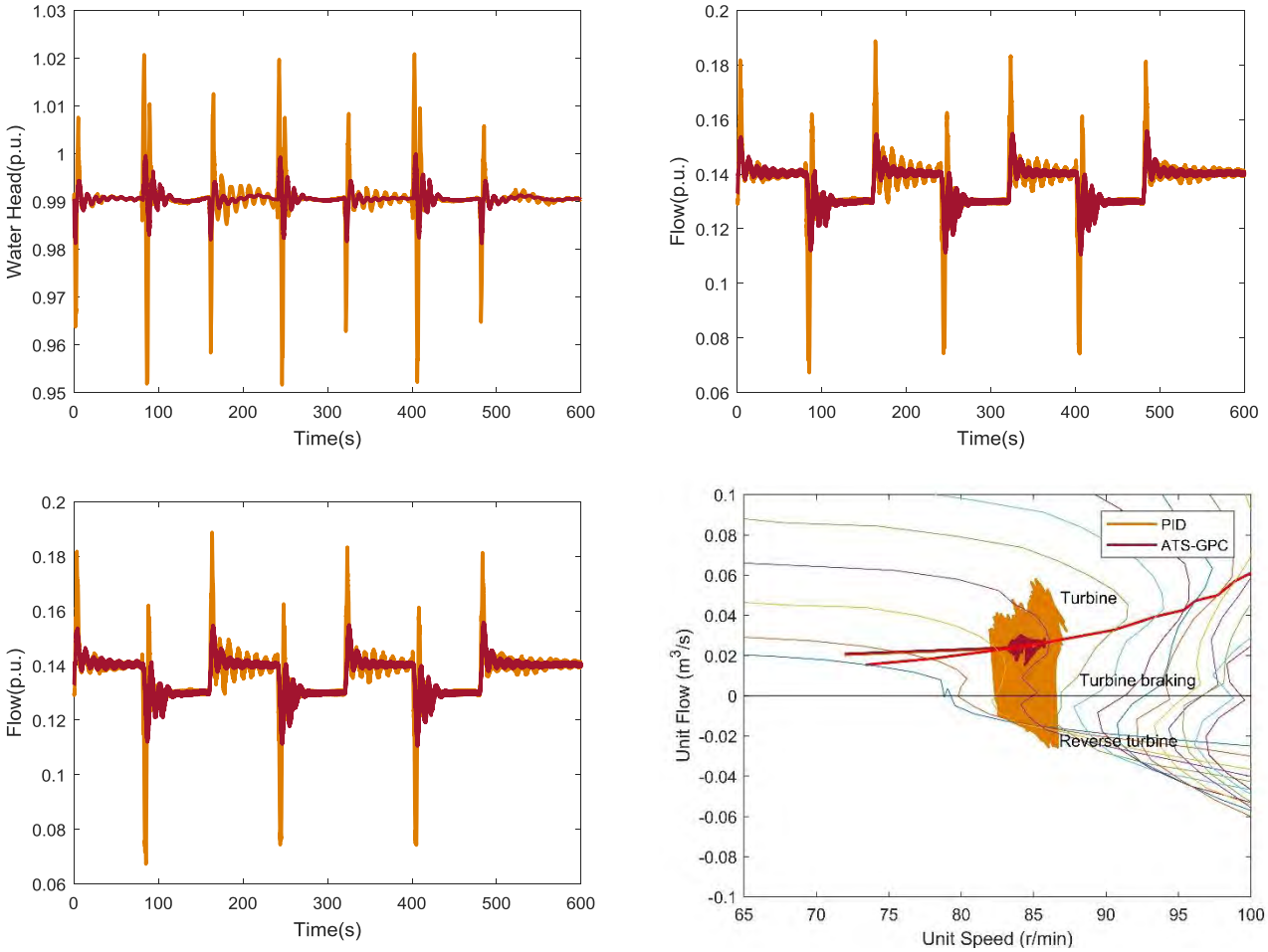

FIGURE 14. Key parameters curves and dynamic process trajectory curves of the PTGS with low water head in square wave signal tracking process.

gain, λ is the forgetting factor. The overall adaptive fuzzy model-based predictive control diagram for PSU is displayed in Fig. 8.

IV. EXPERIMENTS AND DISCUSSION

To verify the performance of the proposed ATS-GPC, the PTGS is simulated in MATLAB, where the ATS-GPC is applied to control the PSU and compare with the traditional PID controller. Further, some simulation experiments including start-up process, speed disturbance process, speed tracking, and robustness analyses are conducted, where all simulation experiments are under no-load condition. The layout type of pressure water supply system is illustrated in Fig.6. The PSU has different dynamic characteristic under different operation heads especially in low head area. In low head area, the PSU is hard to stay stability even lead to unable to synchronize with power grid in turbine start-up. Therefore the three different operation water heads consisted of high water head $H_{\mathrm{H}} = 554$m, middle water head $H_{\mathrm{m}} = 546$, low water head $H_L = 535$m are chosen as the working heads. The corresponding upstream and downstream water level of the PSPS is listed in Table 5.

In order to obtain the controller parameters of the traditional PID, the GSA is used for parameters optimization. The controller parameters $\varpi = [K_p, K_i, K_d]$ is the optimization variables. The parameters of GSA are given as follows: the maximum number of iteration Max_iter $= 200$, the population size $N = 30$, the initial gravitational constant $\mathrm{G}_0 = 20$ and the gravitational constant attenuation factor $\alpha = 6$. In this paper, the integral of the time multiplied absolute error (ITAE) is used as the objective function for the control parameters optimization. The objective function is defined as:

$$f_{ITAE}(\varpi) = \sum_{k=1}^{N_s} T(k) \cdot |(r - x_{\varpi}(k))| \tag{24}$$

where N_s is the number of sampling points, $T(k)$ is the time series, r is the reference frequency, and $x_{\varpi}(k)$ is the unit frequency. The parameter vector ϖ is the optimization variables and the optimal ϖ can be obtained by minimizing the objective function.

To prove that the PID is optimally tuned, the convergence proof of the GSA algorithm is given as following.

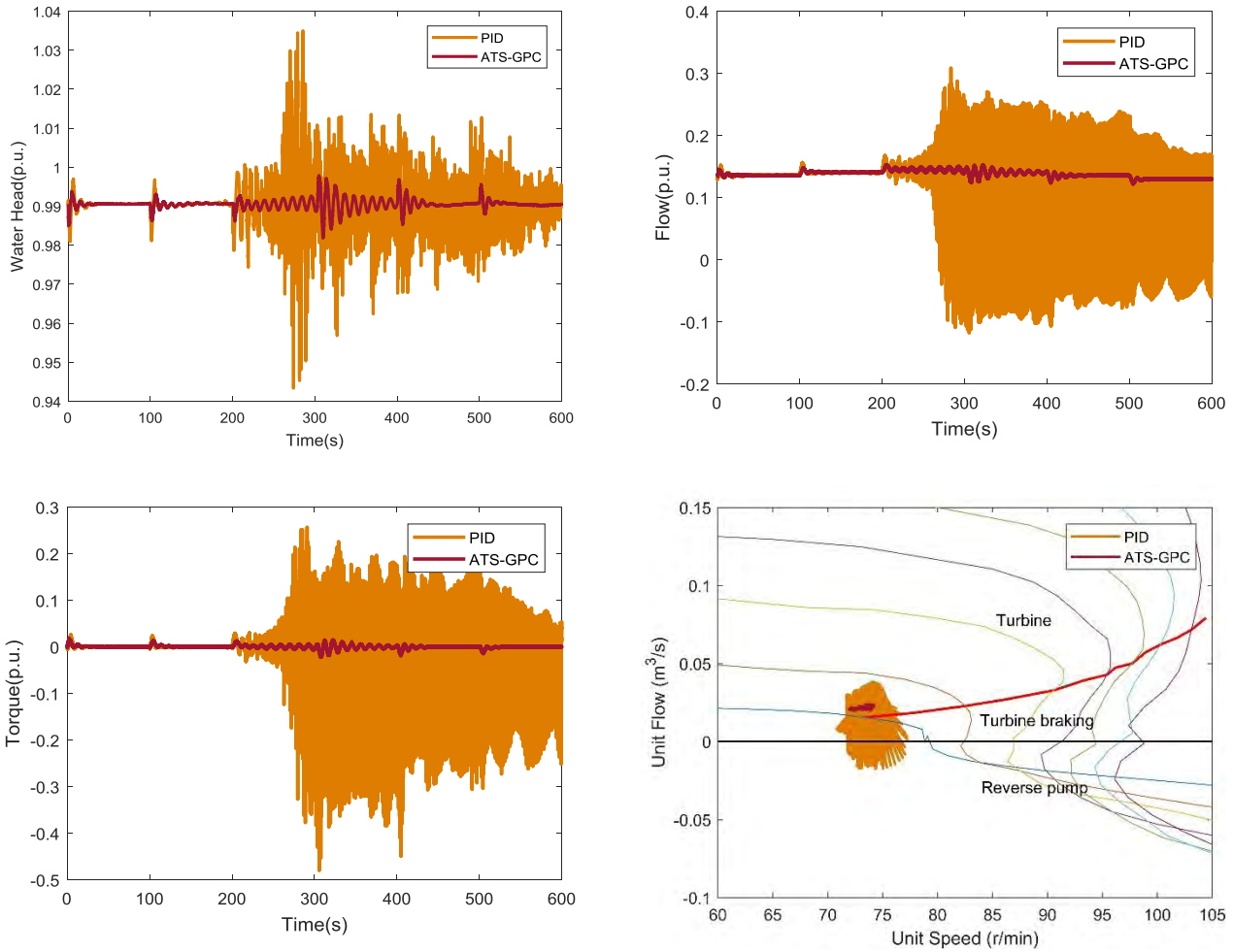

FIGURE 15. Key parameters curves and dynamic process trajectory curves of the PTGS with low water head in step signal tracking process.

Proof: The velocity and position equation of GSA is defined as:

$$\begin{cases} v_i^d(t+1) = r \cdot v_i^d(t) + a_i^d(t) \\ x_i^d(t+1) = x_i^d(t) + v_i^d(t+1) \end{cases} \tag{25}$$

For the Eq. (25), the vectors v and x are the velocity and position of agent i, d is the dimension. The arbitrary dimensions of vectors are independent of each other, so the dimension d is fixed to 1 for simplified proof. The fallowing equation can be deduced based on the Eq. 25:

$$\begin{cases} x(t+2) = x(t+1) + r \cdot v(t+1) + a(t+1) \\ r \cdot x(t+1) = r \cdot x(t) + r \cdot v(t) \end{cases} \tag{26}$$

Subtraction of two formulas in Eq. 26, we can get:

$$x(t+2) - (r+1) \cdot x(t+1) + r \cdot x(t) = a(t+1) \tag{27}$$

It is the second order nonhomogeneous difference equation with constant coefficients. The characteristic equation of the Eq. 27 is:

$$\lambda^2 - (r+1)\lambda + r = 0 \tag{28}$$

Define $\Delta = (1+r)^2 - 4r$, so $\Delta = (1-r)^2 \geq 0$, two situations need to be considered at this point.

(1) when $\Delta = 0$, $\lambda_1 = \lambda_2 = 1$, so $x(t) = (A_0 + A_1 t)\lambda^t$, where A_0 and A_1 are the undetermined coefficients.

(2) when $\Delta > 0$, $\lambda_{1,2} = \frac{r+1 \pm \sqrt{\Delta}}{2}$, so $\lambda_1 = 1$, $\lambda_2 = r$ and $x(t) = A_0 + A_1\lambda_1^t + A_2\lambda_2^t$, where A_0, A_1 and A_2 are the undetermined coefficients.

In GSA algorithm, the r is a random variable in (0,1), therefore $\Delta = (1-r)^2 > 0$ and $x(t) = A_0 + A_1\lambda_1^t + A_2\lambda_2^t$, the limit of the x($t$) is:

$$\lim_{t \to \infty} x(t) = A_0 + A_1 \tag{29}$$

So the particle's trajectory in GSA is convergent and the convergence of the GSA is proved. In the PID controller tuning, the PID controller parameter is the particle's position vector of GSA, so the PID is optimally tuned, i.e. the parameters used are the best in this paper.

A. MODELING OF THE PTGS BASED ON T–S FUZZY MODEL IDENTIFICATION

In this part, the data-derived model of the PTGS is established based on the T-S fuzzy model identification. Some structure

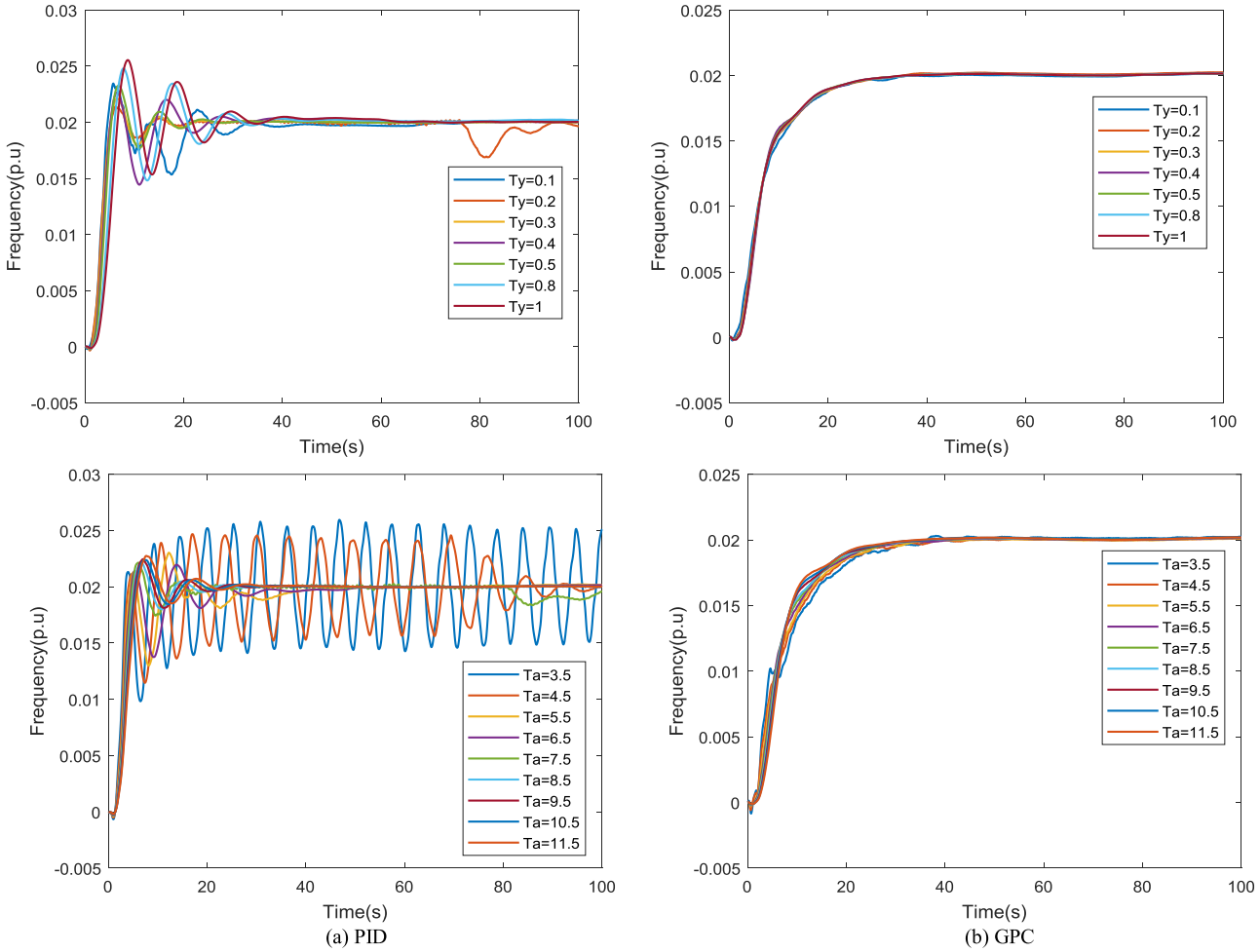

FIGURE 16. Robustness analysis of rotational speed for obtained solution of PID and ATS-GPC under Hw = 554 m.

parameters of the T-S fuzzy model should be determined. The number of fuzzy rules is set to be 3 ($c = 3$). The order of the control signal and the output are set to be 3 (n_y=n_u=3). The mixed sinusoid signal is used as the excited signal. We collect more than 8000 data pairs (u,y) as the original system data. The fuzzy input data and the output data are built by reorganizing the original system data pairs. The fuzzy model has seven input variables $u(k)$, $u(k\text{-}1)$, $u(k\text{-}2)$, $u(k\text{-}3)$, $y(k\text{-}1)$, $y(k\text{-}2)$ and $y(k\text{-}3)$ and a single output variable $y(k)$.

After collecting the data for T-S fuzzy model identification, the classical fuzzy C-means clustering algorithm is used to cluster the data. And then the clustering center and width of every sub-model can be calculated. Finally, the initial consequent parameter is estimated by the recursive least squares method. The output of the original system and the T-S fuzzy model of training data and testing data are compared in Fig. 9(a), and the error is shown in Fig 9(b). From Fig. 9, the T-S fuzzy model shows higher modeling accuracy.

B. START-UP PROCESS

In this part, the no-load start-up process control is considered to test the performance of the proposed ATS-GPC.

The optimized PID controller parameters under different working condition are listed in Table 6, which also shows the parameters of the ATS-GPC. The dynamic speed response of the start-up process under different controllers are shown in Fig. 10. And the corresponding performance indicators including the overshoot (OS), the stable time (ST) and steady-state error (SSE) are reported in Table 7, in which the better results are in a bold. Form Fig. 10 and Table 7, the ATS-GPC shows better control performance for PSU than the traditional PID controller, especially in overshoot and stable time aspects. It means that the proposed ATS-GPC is able to improve the dynamic performance of PSU under no-load start-up process at different water heads.

C. FREQUENCY DISTURBANCE PROCESS

The frequency disturbance experiment are conducted in this part and the PSU also operates under the no-load condition. A step disturbance signal of 2% rated speed is adapted to excite the PTGS. The optimized PID controller parameters under different working condition are listed in Table 8. The simulation results of the frequency disturbance experiment

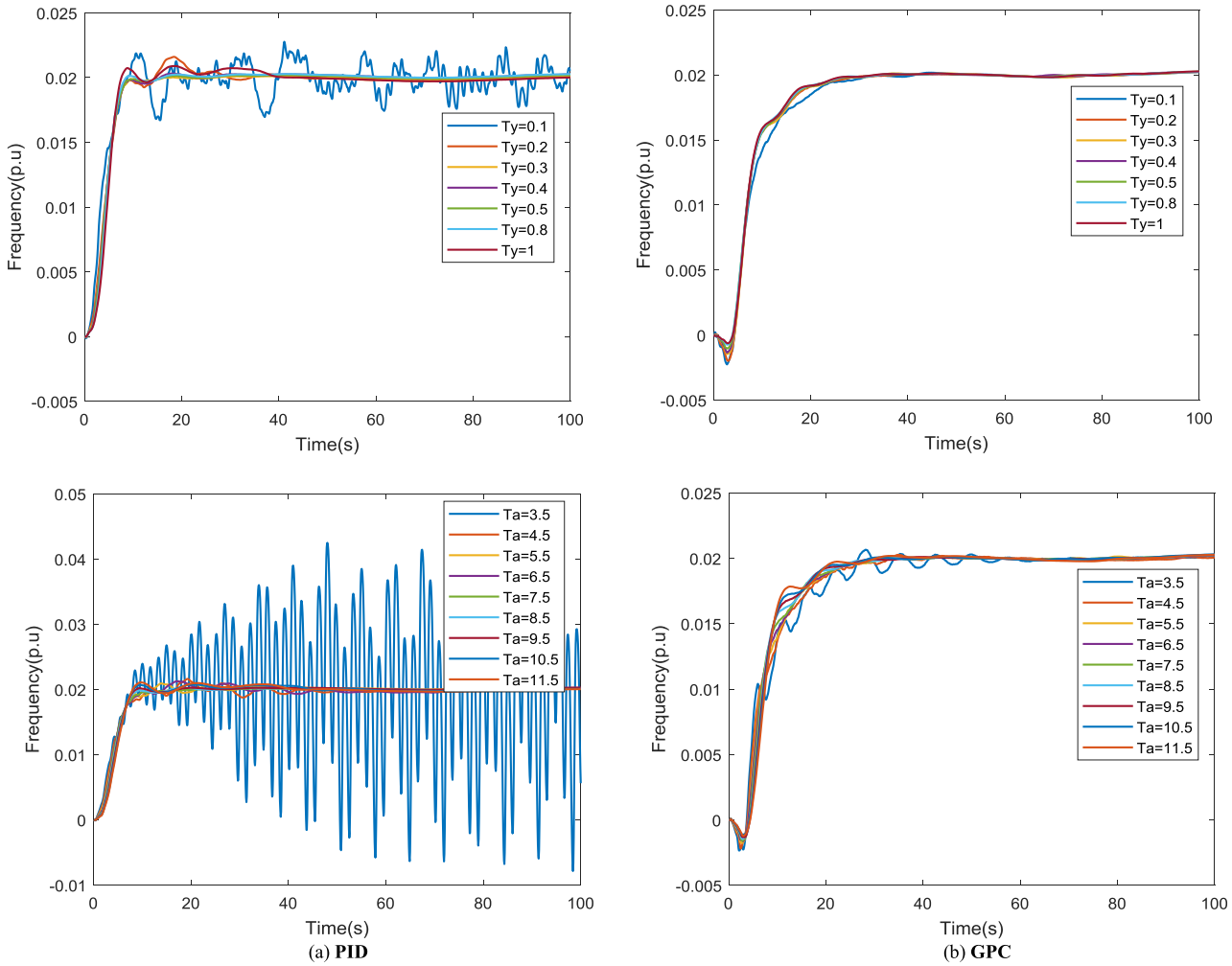

FIGURE 17. Robustness analysis of rotational speed for obtained solution of PID and ATS-GPC under Hw = 546 m.

are illustrated in Fig. 11. The experiments results show that the traditional PID controller is more sensitive to changes in working water heads, but the proposed ATS-GPC can obtain stable good control performance in different operation water heads. Despite that the proposed ATS-GPC has a longer adjustment time than PID, this controller shows better control stability, especially in low water head from the Fig. 11(c). The ATS-GPC significantly enhances the dynamic process of PSU under no-load frequency disturbance condition at low water heads area.

D. FREQUENCY TRACKING EXPERIMENTS

In this part, the square wave signal and the step signal with variable amplitude are used as the reference signal to test the tracking ability of the proposed ATS-GPC. The system output under different water heads by applying the traditional PID controller and the ATS-GPC controller are illustrated in Figs. 12-13. The obtained results show that the proposed ATS-GPC controller effectively controls the system output at the desired reference signal and has obtained better control performance than PID controller under different water heads. Despite that the ATS-GPC is slower than the PID controller, it is able to track the reference signal more smoothly. The system output of the PID controller occurs high frequency oscillation under low water heads, but the ATS-GPC shows smaller vibration amplitude and vibration frequency.

To further explore the control effect of the ATS-GPC in low water head area, the dynamic response curves of the water hammer, the flow, the torque and the dynamic process trajectory curve are illustrated in Figs. 14-15. Clearly, the results indicate that the water hammer, the flow and the torque of the PSU by using the ATS-GPC controller has smaller fluctuations in low water head area. Form the Fig. 13(d) and 15(d), it is clearly shown that the PSU by using the PID controller switches conditions frequently between the turbine mode, turbine barking and the reverse pump mode. The sudden changes in pressure, flow, speed and torque with unpredictable superposition of pressure fluctuation may bring resonance, even result in hydraulic equipment damages. However, the PSU controlled by the proposed ATS-GPC can be stable and converge to one small area at the

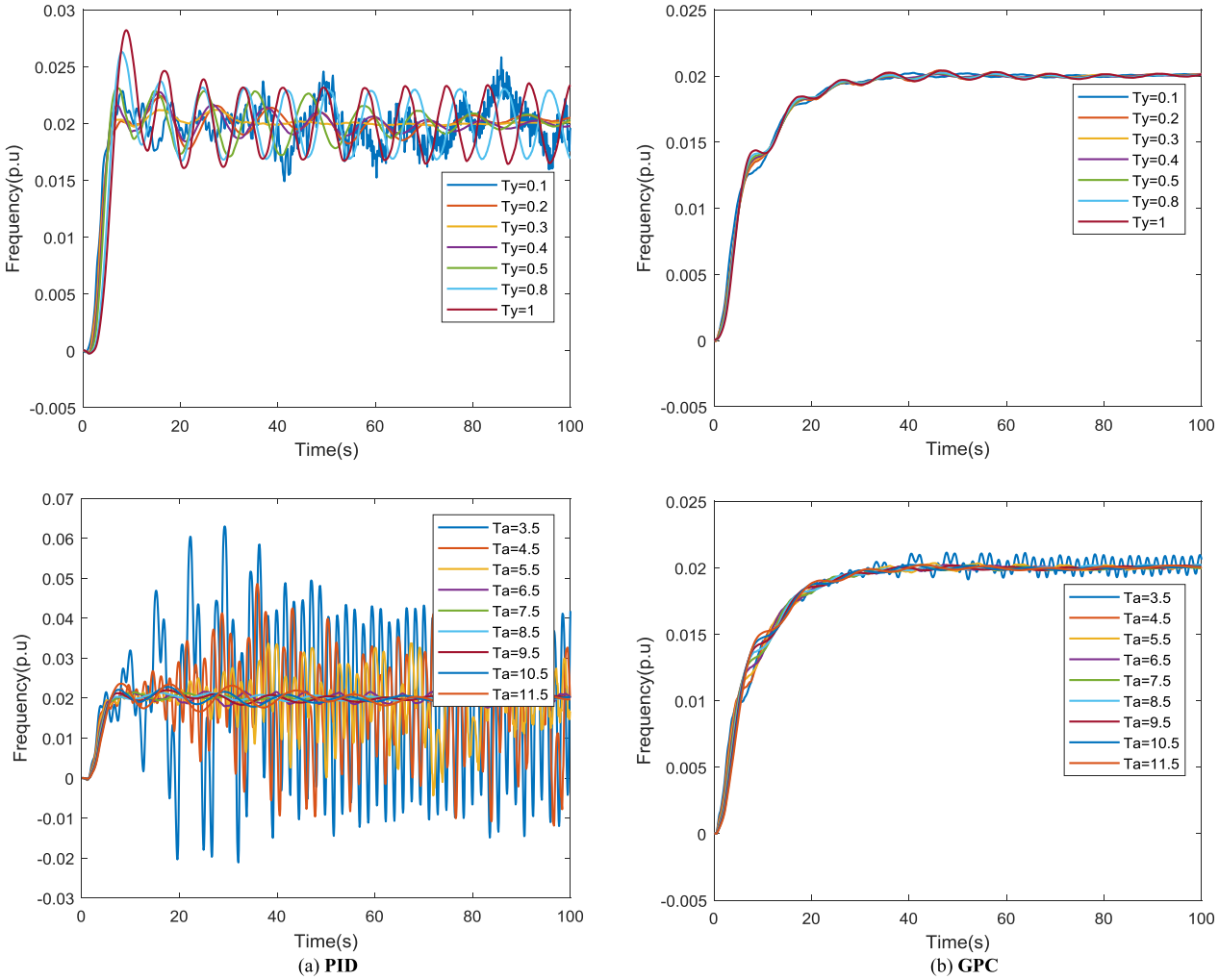

FIGURE 18. Robustness analysis of rotational speed for obtained solution of PID and ATS-GPC under Hw = 535 m.

TABLE 9. Robustness analysis of rotational speed of PID and ATS-GPC on the time constant Ty under Hw = 535 m.

Controller	Performance measure of rotational speed			
	ITAE	OS(%)	ST(s)	SSE(%)
PID	91.28345	29.19208	99.84	0.038594
	37.75803	12.01939	67.36	0.05164
	9.914157	6.056188	28.8	0.011549
	31.50785	13.8205	54.48	0.020695
	57.10306	15.51397	69.68	0.034963
	124.9763	31.46098	100	0.304082
	138.6954	41.05619	100	0.339097
ATS-GPC	18.64517	1.200486	22.72	0.00855
	21.57127	2.108638	23.52	0.010361
	18.52751	0.841193	23.6	0.015897
	17.90358	0.679227	23.68	0.012873
	18.29689	1.02473	23.6	0.008073
	18.41792	1.272336	23.44	0.00812
	21.20367	2.08598	23.28	0.010645

turbine condition. It is obviously seen that the method proposed in this paper can avoid the fluctuation of pressure, flow, speed and torque in the low head area and effectively improve the stability of the PSU.

E. ROBUNESS ANALYSIS

In this part of experiment, the effectiveness of the tuned controller will be tested for sudden-changed operating conditions, i.e. the robustness ability to change in system

TABLE 10. Robustness analysis of rotational speed of PID and ATS-GPC on the time constant Ta under Hw = 535 m.

Controller	Performance measure of rotational speed			
	ITAE	OS(%)	ST(s)	SSE(%)
PID	1051.001	214.9754	100	2.180682
	656.3047	142.8652	99.84	0.045363
	385.469	85.96056	100	0.3259
	63.06099	12.1158	99.12	0.006308
	14.7577	7.25696	22.4	0.005111
	20.29681	6.631367	27.92	0.00441
	28.47053	9.944264	45.68	0.018109
	34.09483	14.11538	49.04	0.032662
	55.13741	18.11309	75.76	0.032242
ATS-GPC	40.16941	5.753124	78.16	0.062898
	19.19359	1.139708	23.76	0.006919
	21.74064	1.785871	24.8	0.017551
	18.8082	1.15419	22.56	0.004054
	19.10452	1.181581	22.8	0.001849
	20.03904	1.16376	23.6	0.023033
	19.39174	0.923117	24.32	0.008869
	19.22942	1.148666	24.96	0.014845
	19.32886	1.110335	24.64	0.006209

TABLE 11. The MSE betweent the origianl indicators and the changing indicators on the time constant Ty under Hw = 535 m.

Controller	Conditions	Correlation coefficient					
PID	T1	135.4533	1480.859	26.5055	8.5149	147.9963	173.623
	T2	2753.622	63.0056	2.2037	0.2292	3.0174	17.3272
	T3	3051.186	575.4332	296.5609	997.1967	4792.017	5786.814
ATS-GPC	T1	**0.1591**	**4.2868**	**0.1267**	**0.1092**	**0.1245**	**0.2509**
	T2	**3.5449**	**0.2473**	**0.4606**	**0.2122**	**0.3317**	**0.3907**
	T3	**0.2631**	**2.7385**	**0.1112**	**0.06**	**0.0937**	**2.2207**

TABLE 12. The MSE betweent the origianl indicators and the changing indicators on the time constant TA under Hw = 535 m.

Controller	Conditions	Correlation coefficient							
PID	T1	12324.18	4434.355	141.6378	36.0826	1915.92	0.9367	0.9702	3.977
	T2	102444	161.5593	4.1082	67.8692	**0.4119**	0.3534	10.9082	23.3375
	T3	280698.7	107060.6	36274.44	1732.076	15.3862	98.418	173.6115	909.075
ATS-GPC	T1	**22.7234**	**1.9462**	**1.3535**	**0.3012**	**0.3026**	**0.2817**	**0.8173**	**0.2871**
	T2	**56.2011**	**3.4739**	**1.4668**	**1.1079**	0.9006	**0.0171**	**0.0407**	**0.2495**
	T3	**851.7652**	**0.3475**	**1.1994**	**0.8743**	**0.6589**	**0.3742**	**0.6682**	**0.5741**

parameters. The variation of the time constant of the main servomotor T_y and the inertial time constant of the generator T_a are considered to carry on for the robustness analysis simulation experiments under different water heads.

The frequency disturbance under no-load conditions is considered in this part for robustness analysis. Figs. 16-18 show the results of the robustness analysis simulation experiment for the traditional PID controller and the proposed ATS-GPC controller in increase and decrease of the time constant T_y and T_a. And the corresponding performance indicators varying with the T_y and T_a under 535m water head are reported in Tables 9-10. The results have shown that no matter how to decrease or increase of the time constant T_y and T_a, the proposed ATS-GPC is able to tolerate these system parameter changes and obtain good control effect under different water heads. However, the traditional PID control is very sensitive to the system parameter changes and has failed to control the PSU, especially in the low water head area. To further explore the changes of the performance indicators varying with the T_y and T_a as reported in Tables 9-10, the mean square error (MSE) between the original performance indicators and the changing performance indicators are shown in Tables 11-12. The Tables 11-12 shown that the variation of the performance indictors by using proposed ATS-GPC is small varying with the T_y and T_a. It is obvious that the proposed ATS-GPC show stronger robustness in system parameters changes under no-load frequency disturbance conditions.

V. CONCLUSION

In this paper, an adaptive Takagi–Sugeno fuzzy model-based generalized predictive controller (ATS-GPC) is proposed for pumped storage unit (PSU). First, the T-S fuzzy model identification is applied to approximate the dynamic characteristics of the established accurate pump-turbine governing system (PTGS). In this approach, the fuzzy C-means clustering algorithm is used to identify the antecedent parameters, and the consequent parameters are calculated by the least

square method. The T-S fuzzy model shows higher modeling accuracy from the experiments results. Second, the adaptive T–S fuzzy model composed of the offline model training and the online consequent parameters adjustment is integrated with the generalized predictive controller to control the PSU. Experiments including start-up process, frequency disturbance process, frequency tracking experiments and robustness analyses have been conducted to verify the proposed method. A comparative analysis has been made between the proposed controller and the traditional PID controller. From these experiments results, it is shown that proposed ATS-GPC is more effective than the traditional PID controller for the improvement of the control performance of the PSU. Although the proposed ATS-GPC has obtained better effect than the traditional PID, it has higher time complexity. Therefore how to reduce the time complexity of the proposed ATS-GPC for PSU deserves further study.

REFERENCES

[1] S. Ahmad and R. M. Tahar, "Selection of renewable energy sources for sustainable development of electricity generation system using analytic hierarchy process: A case of Malaysia," *Renew. Energy*, vol. 63, pp. 458–466, Mar. 2014.
[2] F. Behrouzi, M. Nakisa, A. Maimun, and Y. M. Ahmed, "Global renewable energy and its potential in Malaysia: A review of Hydrokinetic turbine technology," *Renew. Sustain. Energy Rev.*, vol. 62, pp. 1270–1281, Sep. 2016.
[3] A. T. Gullberg, D. Ohlhorst, and M. Schreurs, "Towards a low carbon energy future—Renewable energy cooperation between Germany and Norway," *Renew. Energy*, vol. 68, pp. 216–222, Aug. 2014.
[4] W. Fu, K. Wang, C. Li, and J. Tan, "Multi-step short-term wind speed forecasting approach based on multi-scale dominant ingredient chaotic analysis, improved hybrid GWO-SCA optimization and ELM," *Energy Convers. Manage.*, vol. 187, pp. 356–377, May 2019.
[5] W. Fu, K. Wang, J. Zhou, Y. Xu, J. Tan, and T. Chen, "A hybrid approach for multi-step wind speed forecasting based on multi-scale dominant ingredient chaotic analysis, KELM and synchronous optimization strategy," *Sustainability*, vol. 11, no. 6, p. 1804, Mar. 2019.
[6] M. S. Al-Soud and E. S. Hrayshat, "A 50 MW concentrating solar power plant for Jordan," *J. Cleaner Prod.*, vol. 17, no. 6, pp. 625–635, Apr. 2009.
[7] Y. Xu, C. Li, Z. Wang, N. Zhang, and B. Peng, "Load frequency control of a novel renewable energy integrated micro-grid containing pumped hydropower energy storage," *IEEE Access*, vol. 6, pp. 29067–29077, 2018.
[8] S. V. Papaefthymiou and S. A. Papathanassiou, "Optimum sizing of wind-pumped-storage hybrid power stations in island systems," *Renew. Energy*, vol. 64, pp. 187–196, Apr. 2014.
[9] J. A. M. Sousa, F. Teixeira, and S. Faias, "Impact of a price-maker pumped storage hydro unit on the integration of wind energy in power systems," *Energy*, vol. 69, pp. 3–11, May 2014.
[10] Z. Zuo, H. Fan, S. Liu, and Y. Wu, "S-shaped characteristics on the performance curves of pump-turbines in turbine mode—A review," *Renew. Sustain. Energy Rev.*, vol. 60, pp. 836–851, Jan. 2016.
[11] Z. Zuo, S. Liu, Y. Sun, and Y. Wu, "Pressure fluctuations in the vaneless space of high-head pump-turbines—A review," *Renew. Sustain. Energy Rev.*, vol. 41, pp. 965–974, Jan. 2015.
[12] W. Fu, K. Wang, C. Li, X. Li, Y. Li, and H. Zhong, "Vibration trend measurement for a hydropower generator based on optimal variational mode decomposition and an LSSVM improved with chaotic sine cosine algorithm optimization," *Meas. Sci. Technol.*, vol. 30, no. 1, Dec. 2018, Art. no. 015012.
[13] J. Li, Q. Hu, J. Yu, and Q. Li, "Study on S-shaped characteristic of Francis reversible unit by on-site test and CFD simulation," *Sci. China Technol. Sci.*, vol. 56, no. 9, pp. 2163–2169, Sep. 2013.
[14] W. Zeng, J. D. Yang, Y. G. Cheng, and W. C. Guo, "Formulae for the intersecting curves of pump-turbine characteristic curves with coordinate planes in three-dimensional parameter space," *Proc. Inst. Mech. Eng. A, J. Power Energy*, vol. 229, no. 3, pp. 324–336, Feb. 2015.
[15] S. Pejovic, L. Krsmanovic, R. Jemcov, and P. Crnkovic, "Unstable operation of high-head reversible pump-turbines," in *Proc. 8th IAHR Symp. Hydraulic Mach. Cavitation*, Leningrad, USSR, 1976, pp. 283–295.
[16] R. J. Swed and K. H. Yang, "Experiences on startup and trial operation at Yards Creek pumped storage project," *J. Basic Eng.*, vol. 91, no. 3, pp. 387–395, Sep. 1969.
[17] S. Pejovic, Q. F. Zhang, B. Karney, and A. Gajic, "Analysis of pump-turbine 'S' instability and reverse water hammer incidents in hydropower systems," in *Proc. 4th Int. Meeting Cavitation Dyn. Problems Hydraulic Mach. Syst.*, Oct. 2011, pp. 26–28.
[18] C. Li, N. Zhang, X. Lai, J. Zhou, and Y. Xu, "Design of a fractional-order PID controller for a pumped storage unit using a gravitational search algorithm based on the cauchy and Gaussian mutation," *Inf. Sci.*, vol. 396, pp. 162–181, Aug. 2017.
[19] Y. Xu, J. Zhou, X. Xue, W. Fu, W. Zhu, and C. Li, "An adaptively fast fuzzy fractional order PID control for pumped storage hydro unit using improved gravitational search algorithm," *Energy Convers. Manage.*, vol. 111, pp. 67–78, Mar. 2016.
[20] X. Yuan, Z. Chen, Y. Yuan, and Y. Huang, "Design of fuzzy sliding mode controller for hydraulic turbine regulating system via input state feedback linearization method," *Energy*, vol. 93, pp. 173–187, Dec. 2015.
[21] X. Yuan, Z. Chen, Y. Yuan, Y. Huang, X. Li, and W. Li, "Sliding mode controller of hydraulic generator regulating system based on the input/output feedback linearization method," *Math. Comput. Simul.*, vol. 119, pp. 18–34, Jan. 2016.
[22] S. Balochian and S. Vosoughi, "Design and simulation of turbine speed control system based on adaptive fuzzy PID controller," *Adv. Mech. Eng. Appl.*, vol. 1, no. 3, pp. 2167–6380, 2012.
[23] D. J. King, D. A. Bradley, S. P. Mansoor, D. I. Jones, F. C. Aris, and G. R. Jones, "Using a fuzzy inference system to control a pumped storage hydro plant," in *Proc. 10th IEEE Int. Conf. Fuzzy Syst.*, Dec. 2001, pp. 1008–1011.
[24] C. Li, Y. Mao, J. Zhou, N. Zhang, and X. An, "Design of a fuzzy-PID controller for a nonlinear hydraulic turbine governing system by using a novel gravitational search algorithm based on cauchy mutation and mass weighting," *Appl. Soft Comput.*, vol. 52, pp. 290–305, Mar. 2017.
[25] C. Li, Y. Mao, J. Yang, Z. Wang, and Y. Xu, "A nonlinear generalized predictive control for pumped storage unit," *Renew. Energy*, vol. 114, pp. 945–959, Dec. 2017.
[26] Y. Xu, Y. Zheng, Y. Du, W. Yang, X. Peng, and C. Li, "Adaptive condition predictive-fuzzy PID optimal control of start-up process for pumped storage unit at low head area," *Energy Convers. Manage.*, vol. 177, pp. 592–604, Dec. 2018.
[27] M. Darabian, A. Jalilvand, and M. Azari, "Power system stability enhancement in the presence of renewable energy resources and HVDC lines based on predictive control strategy," *Int. J. Elect. Power Energy Syst.*, vol. 80, pp. 363–373, Sep. 2016.
[28] S. J. Qin and T. A. Badgwell, "A survey of industrial model predictive control technology," *Control Eng. Pract.*, vol. 11, no. 7, pp. 733–764, Jul. 2003.
[29] M. Romero, A. P. de Madrid, C. Mañoso, and V. Milanés, "Low speed hybrid generalized predictive control of a gasoline-propelled car," *ISA Trans.*, vol. 57, pp. 373–381, Jul. 2015.
[30] J. Zhang, Y. Zhou, Y. Li, G. Hou, and F. Fang, "Generalized predictive control applied in waste heat recovery power plants," *Appl. Energy*, vol. 102, pp. 320–326, Feb. 2013.
[31] N. Kishor and S. P. Singh, "Simulated response of NN based identification and predictive control of hydro plant," *Expert Syst. Appl.*, vol. 32, no. 1, pp. 233–244, 2007.
[32] I. Boulkaibet, K. Belarbi, S. Bououden, T. Marwala, and M. Chadli, "A new T-S fuzzy model predictive control for nonlinear processes," *Expert Syst. Appl.*, vol. 88, pp. 132–151, Dec. 2017.
[33] L. Cheng, W. Liu, Z.-G. Hou, T. Huang, J. Yu, and M. Tan, "An adaptive Takagi–Sugeno fuzzy model-based predictive controller for piezoelectric actuators," *IEEE Trans. Ind. Electron.*, vol. 64, no. 4, pp. 3048–3058, Apr. 2017.
[34] B. Ding, "Dynamic output feedback predictive control for nonlinear systems represented by a Takagi–Sugeno model," *IEEE Trans. Fuzzy Syst.*, vol. 19, no. 5, pp. 831–843, Oct. 2011.
[35] W. Yang, G. Feng, and T. Zhang, "Robust model predictive control for discrete-time Takagi–Sugeno fuzzy systems with structured uncertainties and persistent disturbances," *IEEE Trans. Fuzzy Syst.*, vol. 22, no. 5, pp. 1213–1228, Oct. 2014.

[36] C. Li, L. Chang, Z. Huang, Y. Liu, and N. Zhang, "Parameter identification of a nonlinear model of hydraulic turbine governing system with an elastic water hammer based on a modified gravitational search algorithm," *Eng. Appl. Artif. Intell.*, vol. 50, pp. 177–191, Apr. 2016.
[37] C. Li and J. Zhou, "Parameters identification of hydraulic turbine governing system using improved gravitational search algorithm," *Energ. Convers. Manage.*, vol. 52, no. 1, pp. 374–381, Jan. 2011.
[38] Z. Wang, C. Li, X. Lai, N. Zhang, Y. Xu, and J. Hou, "An integrated start-up method for pumped storage units based on a novel artificial sheep algorithm," *Energies*, vol. 11, no. 1, p. 151, Jan. 2018.
[39] N. Zhang, C. Li, R. Li, X. Lai, and Y. Zhang, "A mixed-strategy based gravitational search algorithm for parameter identification of hydraulic turbine governing system," *Knowl.-Based Syst.*, vol. 109, pp. 218–237, Oct. 2016.
[40] H. Fang, L. Chen, N. Dlakavu, and Z. Shen, "Basic modeling and simulation tool for analysis of hydraulic transients in hydroelectric power plants," *IEEE Trans. Energy Convers.*, vol. 23, no. 3, pp. 834–841, Sep. 2008.
[41] X. Lai, C. Li, J. Zhou, and N. Zhang, "Multi-objective optimization for guide vane shutting based on MOASA," *Renew. Energy*, vol. 139, pp. 302–312, Aug. 2019.
[42] K. Vereide, B. Svingen, T. K. Nielsen, and L. Lia, "The effect of surge tank throttling on governor stability, power control, and hydraulic transients in hydropower plants," *IEEE Trans. Energy Convers.*, vol. 32, no. 1, pp. 91–98, Mar. 2017.
[43] J. Hou, C. Li, Z. Tian, Y. Xu, X. Lai, N. Zhang, T. Zheng, and W. Wu, "Multi-objective optimization of start-up strategy for pumped storage units," *Energies*, vol. 11, no. 5, p. 1141, May 2018.
[44] X.-J. Liu and C. W. Chan, "Neuro-fuzzy generalized predictive control of boiler steam temperature," *IEEE Trans. Energy Convers.*, vol. 21, no. 4, pp. 900–908, Dec. 2006.
[45] G. A. M. Muoz-Hernndez and D. Jones, "MIMO generalized predictive control for a hydroelectric power station," *IEEE Trans. Energy Convers.*, vol. 21, no. 4, pp. 921–929, Dec. 2006.
[46] C. Li, J. Zhou, L. Chang, Z. Huang, and Y. Zhang, "T–S fuzzy model identification based on a novel hyperplane-shaped membership function," *IEEE Trans. Fuzzy Syst.*, vol. 25, no. 5, pp. 1364–1370, Oct. 2017.
[47] C. Li, J. Zhou, B. Fu, P. Kou, and J. Xiao, "T–S fuzzy model identification with a gravitational search-based hyperplane clustering algorithm," *IEEE Trans. Fuzzy Syst.*, vol. 20, no. 2, pp. 305–317, Apr. 2012.
[48] W. Zou, C. Li, and N. Zhang, "A T–S fuzzy model identification approach based on a modified inter type-2 FRCM algorithm," *IEEE Trans. Fuzzy Syst.*, vol. 26, no. 3, pp. 1104–1113, Jun. 2018.

JIANZHONG ZHOU was born in Wuhan, China, in December 1959. He received the B.S. degree in automatic control from the Nanjing University of Aeronautics and Astronautics, Nanjing, China, in 1982. He is currently a Professor with the School of Hydropower and Information Engineering, Huazhong University of Science and Technology. His research interests include modeling, control, and operation theory in hydraulic power plants.

NAN ZHANG received the B.S. degree in electronic information engineering from Wuhan Textile University, Wuhan, China, in 2014. He is currently pursuing the Ph.D. degree in water conservancy and hydropower engineering with the Huazhong University of Science and Technology. His research interests include control theory, system identification, and modeling of power generation systems.

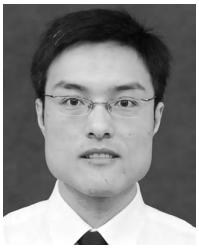

CHAOSHUN LI received the B.S. degree in thermal energy and power engineering from Wuhan University, Wuhan, China, in 2005, and the Ph.D. degree in water conservancy and hydropower engineering from the Huazhong University of Science and Technology, in 2010, where he is currently an Associate Professor with the School of Hydropower and Information Engineering. His research interests include fuzzy application systems, fuzzy modeling, and system identification.

YONGCHUAN ZHANG was born in Henan, China, in March 1935. He is currently an Academician with the Chinese Academy of Engineering and a Professor with the Hydropower and Automation Engineering Department, Huazhong University of Science and Technology. His major research interests include digital cascaded hydroelectric systems and its optimal dispatching.

XINJIE LAI received the B.S. degree in hydraulic and hydroelectric engineering from the Huazhong University of Science and Technology (HUST), Wuhan, China, in 2016, where he is currently pursuing the Ph.D. degree with the School of Hydropower and Information Engineering. His research interests include system indentification, advanced control theory, and adaptive control of hydropower units connecting to the power grid.